ARTICLES

Diffuse x-ray scattering of Ag–13.4 at. % Al

S. Y. Yu, B. Schönfeld, and G. Kostorz
Institut für Angewandte Physik, Eidgenössische Technische Hochschule Zürich, CH-8093 Zürich, Switzerland
(Received 31 March 1997)

A single crystal of Ag–13.4 at. % Al aged within the α phase at 673 K was investigated by diffuse x-ray scattering. The separated short-range-order scattering is only weakly modulated and shows two types of diffuse maxima simultaneously, at $2k_F^{110}$ (where k_F is the Fermi wave number along $\langle 110 \rangle$) and at 1/2,1/2,1/2 positions. Such a topology has previously been observed only in the Cu-Pt system. A detailed analysis of nearest-neighbor configurations, however, exhibits large differences between the two systems; the data suggest the A_5B structure as a possible ground-state structure of the fcc Ag-Al lattice, i.e., none of the structures observed in the Cu-Pt system. For this structure an order-disorder transition temperature of $\sim$135 K is estimated on the basis of Monte Carlo simulations with effective pair-interaction parameters of the first 18 shells. [S0163-1829(97)02938-X]

INTRODUCTION

Short-range order in fcc Ag-rich Ag-Al (α phase) has been known for some time from the results of diffuse scattering and measurements of the electrical resistivity.[1,2] Recently, Kulish and Petrenko[3] investigated polycrystalline Ag-Al by diffuse x-ray scattering with the samples held at the aging temperature as well as following a subsequent quench to room temperature. The data presented in detail for Ag–15 at. % Al were fitted to a small number of Fourier coefficients (four short-range-order parameters and two displacement parameters). As these parameters were found to vary nonmonotonically with the aging temperature, the presence of two types of short-range order or structures were claimed to be present. While at high temperature short-range order should locally resemble the $L1_2$ structure, martensitic β' (for its characterization, see Gupta[4]) should occur at lower temperatures. Two remarks, however, must be made: (i) while the nearest-neighbor short-range-order parameter indicates a low degree of order, an exceptionally high value is found for the second-nearest neighbors. (ii) The data suggesting a nonmonotonic variation with aging temperature were taken not only within the α phase but also within the α-μ two-phase region.

The nearest-neighbor short-range-order parameter α_{110} was also calculated from measurements of the electrical resistivity by Pfeiler *et al.*[5] They assumed (i) a linear dependence of the change of electrical resistivity induced by short-range order on α_{110} and (ii) a temperature-independent proportionality factor. The variation of α_{110} with temperature was considered in a quasichemical model. The data obtained for α_{110} are of the same order as those found by diffuse scattering.

The presence of short-range order had also been noted in the course of the decomposition of Al-rich Al-Ag alloys. Based on small-angle and diffuse wide-angle scattering experiments, Malik *et al.*[6] determined the microstructure of the Guinier-Preston zones and found that the zones of an average composition of Ag-(80$\pm$10) at. % Al are short-range ordered. Values thus obtained for $|\alpha_{110}|$ are larger than those found in the studies quoted above.[3,5]

In conclusion, the knowledge of the pair correlation function in Ag-Al is very limited. For a detailed determination, diffuse scattering from single crystals is required (see, e.g., Ref. 7).

From the pair-correlation function the local atomic arrangements and the effective pair-interaction parameters (if states of thermal equilibrium are investigated) can be deduced. This is of special interest in Al-Ag, as no long-range-ordered (fcc) structure is known directly from experiment. Based on electronic structure calculations, Asta[8] found three ground-state structures and determined their range of existence for a phase diagram relative to the fcc lattice. These are Ag_2Al (Pt_2Mo type), Ag_3Al ($D0_{22}$) and Ag_5Al [A_5B type, see Fig. 1(a)]. For the hcp lattice two long-range-ordered structures have been proposed. Based on x-ray diffraction in highly symmetrical directions from Ag–33 at. % Al single crystals, Neumann[10] suggested a superlattice where in each basal plane an Al atom is surrounded by 6 Ag atoms. No structural predictions could be given to reproduce the slight compositional variation observed for alternating basal planes. The second model was introduced by Howe *et al.*[11] for the structure of γ' precipitates which appear during the decomposition of Al-rich Al-Ag alloys. It is based on results from high-resolution electron microscopy in combination with image simulations, EDS and CBED. Consecutive basal planes are now made either of pure Ag or Al–33 at. % Ag (any Ag atom is surrounded by 6 Al atoms in the basal plane). Both models are shown in Figs. 1(b) and 1(c). First-principles calculations were done by Rohrer *et al.*[12] for both suggested structures. The structure proposed by Howe *et al.* was judged to be more stable.

In the present determination of the microstructure in fcc Ag-Al, a single crystal with 13.4 at. % Al aged at 673 K was

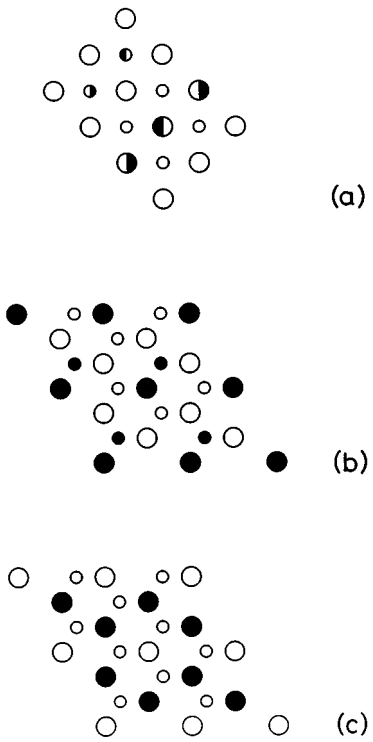

FIG. 1. (a) A_5B structure viewed along [001] direction (Ref. 9). Different sizes refer to successive (001) planes with ○, *A* and ●, *B* atoms always along [001], while alternating site occupancy with *A* and *B* atoms (*B* and *A* atoms) is indicated by half-shaded circles. Ag_2Al structures introduced by (b) Neumann (Ref. 10) and (c) Howe *et al.* (Ref. 11). ○, Ag and ●, Al atoms.

investigated. These conditions were chosen (i) to get a large degree of short-range order because of a large Al fraction and (ii) to have a low aging temperature just above the $\alpha/(\alpha\text{-}\mu)$ phase boundary ($\sim$585 K for 13.4 at. % Al, see Ref. 13). This state should be preserved in quenching to room temperature to allow effective pair-interaction parameters to be deduced and low-temperature ground states to be discussed. X rays were preferred over neutrons in the three-dimensional scattering experiment as the scattering contrast (the difference of the atomic scattering factors normalized to an average scattering length) is then larger by a factor of ~ 2.

THEORY

The elastic coherent diffuse scattering from a single-crystalline alloy arises from any static breaking of the translational invariance of the lattice, such as the mere presence of different types of atoms and the different atomic sizes leading to static atomic displacements. Within the framework of the kinematic theory and in the quadratic approximation of the displacement scattering for a binary *A*-*B* cubic crystal, this diffuse scattering I_{diff} can be written as a sum of short-range-order scattering I_{SRO}, size effect scattering I_{SE}, and Huang scattering I_{H}:

$$I_{\text{diff}}(\underline{h}) = I_{\text{SRO}}(\underline{h}) + I_{\text{SE}}(\underline{h}) + I_{\text{H}}(\underline{h}), \tag{1}$$

where $\underline{h}$ is the scattering vector in reciprocal-lattice units (r.l.u.) ($|\underline{h}| = 2a \sin\theta/\lambda$, θ is half the scattering angle, a is the mean lattice parameter, λ is the wavelength of the incident radiation). The diffuse scattering $I_{\text{diff}}(\underline{h})$ is given in Laue units, $c_A c_B |f_A - f_B|^2$, with c_μ = atomic fraction and f_μ = atomic scattering factor of component μ. Short-range-order scattering $I_{\text{SRO}}(\underline{h})$ is given by

$$I_{\text{SRO}}(\underline{h}) = \sum_{lmn} \alpha_{lmn} \cos(\pi h_1 l)\cos(\pi h_2 m)\cos(\pi h_3 n), \tag{2}$$

where l,m,n are integers defining the interatomic vectors in units of half the lattice parameter a, and α_{lmn} are the Warren-Cowley short-range-order parameters[14]

$$\alpha_{lmn} = 1 - P^{AB}_{lmn}/c_B, \tag{3}$$

with P^{AB}_{lmn} the conditional probability of finding a *B* atom at any site of type lmn if an *A* atom is at position 000.

Short-range-order scattering can be separated from the total diffuse scattering I_{diff} by the separation techniques of Borie and Sparks[15] (BS) and Georgopoulos and Cohen[16] (GC). Both methods are based on the symmetry of the different scattering contributions I_{SRO}, I_{SE}, and I_{H} combined with their different weighting with scattering vector $\underline{h}$. While the BS method assumes no difference in the dependence of the atomic scattering factors f_A and f_B, the GC method is explicitly based on the differences in their $\underline{h}$ dependence. Thus, the BS method is more appropriate for nonmagnetic neutron scattering while for x-ray scattering, the GC method should be used.

EXPERIMENT

A single crystal of Ag with nominally 15 at. % Al, about 90 mm long and 12 mm in diameter, was grown by the Bridgman technique under argon atmosphere in a high-purity graphite crucible. The starting materials were high-purity aluminium (99.999 at. %) of VAW Aluminium (Bonn, Germany) and high-purity silver (99.99 at. %) of Métaux Précieux SA METALOR (Neuchâtel, Switzerland).

The composition of the sample analyzed from adjacent slices by wet-chemical analysis by the Ag supplier was Ag–(13.35±0.03) at. % Al. A cylindrically shaped slice, 11 mm in diameter and 3.2 mm in height with a surface normal near the [421] direction, was cut from the single crystal by spark erosion. The slice was homogenized at 973 K for 1 d and quenched into iced water, subsequently annealed at 673 K for 184 h and again quenched into iced water. The aging temperature was chosen in the α phase[13] close to the α-μ two-phase region to set up a high degree of short-range order. As the relaxation time for short-range ordering extrapolated from the data of Meisterle and Pfeiler[17] (these data were probably partly taken within the α-μ two-phase region) is less than 1 s (estimated value at 573 K), a state of thermal equilibrium might not have been frozen in. To obtain a flat sample surface for the x-ray measurements, the slice was first mechanically polished (final polish with a diamond paste of 3 μm). The damaged surface layer was then electrochemically removed for about 10 s with 1 A current in a solution of 80% phosphoric acid (85%) and 20% nitric acid (65%).

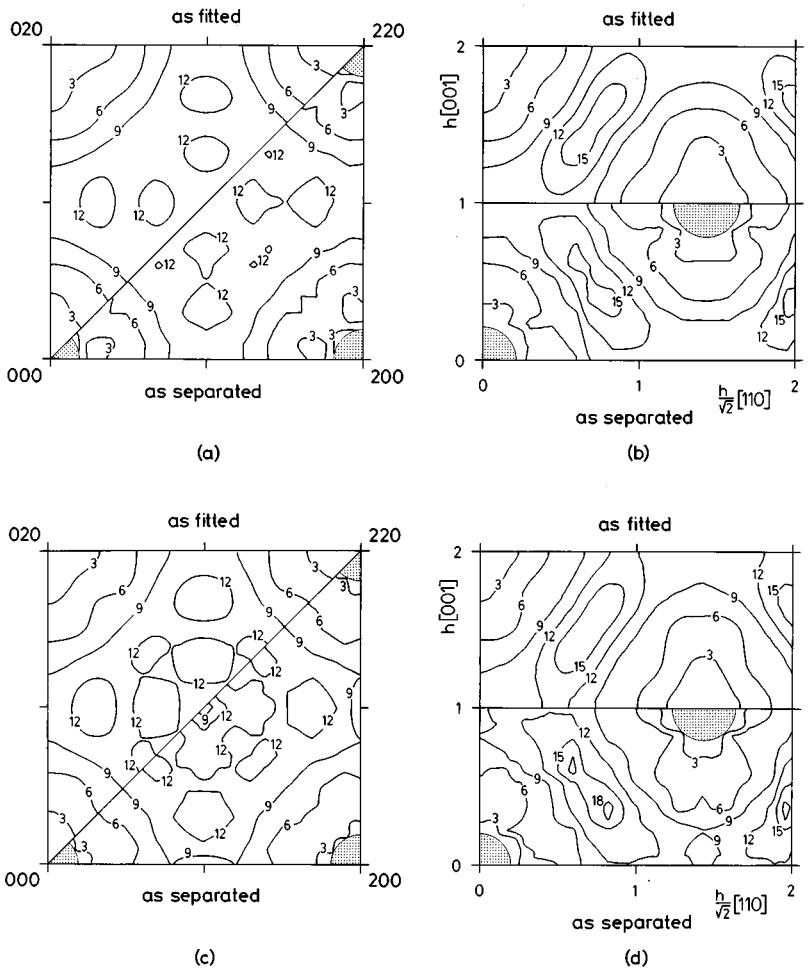

FIG. 2. Lines of equal intensity for $I_{\mathrm{SRO}}(\underline{h})$ in 0.1 Laue units as separated and as recalculated from the 27 α_{lmn} of Table I: (a) (001) and (b) (110) plane (based on the GC separation technique), (c) (001) and (d) (110) plane (based on the BS separation technique).

Diffuse x-ray measurements were carried out on a four-circle diffractometer at room temperature. A Rotaflex RU-200BH (Rigaku, Japan) operated at 180 mA and 50 kV was used as the x-ray source. The Mo K_α radiation ($\lambda = 0.071\,069$ nm) was selected by a doubly bent pyrolytic graphite monochromator. The sample was mounted in an evacuated sample chamber. The diffuse intensity was measured at about 11 000 positions under monitor control. Typically, 4000–12 000 counts were registered per position in about 150 s. A spacing of 0.1 r.l.u. (reciprocal-lattice units $2\pi/a$) was chosen, with scattering vectors ranging from 1.4 to 7.4 r.l.u.

To obtain the elastic scattering from the experimental counts, the scattering was put on an absolute scale by comparison with the scattering from polysterene, and Compton scattering and thermal diffuse scattering were calculated and subtracted. Compton scattering was taken from the data of Cromer[18] for Al and of Cromer and Mann[19] for Ag. Thermal diffuse scattering up to third order was calculated using the elastic constants measured by the ultrasonic pulse-echo-overlap method for a sample of the same composition and thermal history. The elastic constants at room temperature are $c_{11}=121.7(8)$ GPa, $c_{12}=96.8(2)$ GPa, and $c_{44}=46.9(2)$ GPa. From the elastic constants, $B_{\mathrm{t}}=0.733\times10^{-2}$ nm^2 and $B_{\mathrm{s}}=0.014\times10^{-2}$ nm^2 were determined for the thermal and static part of B in the Debye-Waller factor $\exp[-2B\sin(\theta/\lambda)^2]$.[20,21] The atomic scattering factors of Ag and Al were taken from Doyle and Turner[22] and the dispersion corrections from Sasaki.[23]

DIFFUSE SCATTERING

Short-range-order scattering was obtained by the separation methods of Georgopoulos-Cohen[16] and Borie-Sparks.[15] Although the BS method only represents an approximation to the GC scheme for diffuse x-ray scattering, it is a valuable tool in judging any conclusion for the following reasons. First, the difference between the atomic sizes of Ag and Al is small and the approximate treatment of displacement scattering is less crucial. Second, a lower number of Fourier series are required in the BS method, which is advantageous in the present situation where only a small modulation of short-range-order scattering (between 0.2 and 1.8 Laue units) is present.

Figure 2 shows the separated short-range-order scattering within the (100) and (110) planes of reciprocal space obtained with the use of both methods; the dotted areas around the Bragg reflections were not considered in the evaluation because of increased thermal diffuse scattering and possible tails of the Bragg reflections. Two types of diffuse maxima

TABLE I. Warren-Cowley short-range-order parameters α_{lmn} according to the Georgopoulos-Cohen (GC) and the Borie-Sparks (BS) separation techniques.

	α_{lmn}	
lmn	GC	BS
000	0.9732(32)	1.0234(29)
110	−0.0804(13)	−0.0784(11)
200	−0.0523(11)	−0.0562(12)
211	0.0149(6)	0.0146(5)
220	0.0262(7)	0.0258(9)
310	0.0036(6)	0.0019(6)
222	−0.0062(9)	−0.0064(9)
321	−0.0048(5)	−0.0052(4)
400	−0.0060(12)	−0.0057(11)
330	−0.0073(8)	−0.0070(8)
411	−0.0027(6)	−0.0031(6)
420	−0.0013(6)	−0.0019(6)
233	0.0053(7)	0.0048(6)
422	−0.0020(5)	−0.0022(5)
431	0.0036(4)	0.0041(4)
510	−0.0017(7)	−0.0011(6)
521	0.0015(4)	0.0010(4)
440	0.0001(8)	−0.0007(7)
433	−0.0002(6)	0.0007(6)
530	0.0005(5)	−0.0002(6)
244	−0.0003(5)	−0.0008(5)
600	0.0040(11)	0.0034(10)
532	−0.0009(4)	−0.0009(4)
611	−0.0014(6)	−0.0002(5)
620	0.0005(5)	0.0004(5)
541	−0.0001(4)	0.0011(4)
622	0.0004(5)	−0.0006(5)

are observed, a local one at $2k_F^{110}$ positions and an absolute one around 1/2,1/2,1/2. The first type arises because of the flat pieces of the Fermi surface along ⟨110⟩ that are spanned by the scattering vector $2k_F^{110}$. The second type is located close to one of the special points of the fcc lattice. While it is difficult to decide whether there is a split maximum close to 1/2,1/2,1/2 or not (see the subtle differences in the GC and BS analyses), the elongated shape of the lines of equal intensity around this special point is certainly striking. Strong deviations from spherically shaped isointensity lines around special points are known for 100 positions in various binary copper and nickel alloys.[24–27] A correlation between the shape of the contour lines and the presence of antiphase boundaries or a platelike nature of short-range-ordered ''regions'' has been suggested. In the present case, however, the low degree of short-range order makes it impossible to reach any such conclusion from modeling.

The Warren-Cowley short-range-order parameters α_{lmn} were determined by a least-squares-fitting procedure from the short-range-order scattering I_{SRO}. At least 17 values of α_{lmn} are required to reproduce the topology with diffuse maxima around the 1/2, 1/2, 1/2 and $2k_F^{110}$ positions. Judging the quality of the fit from its weighted R value, and especially from the intensity distribution around the two types of

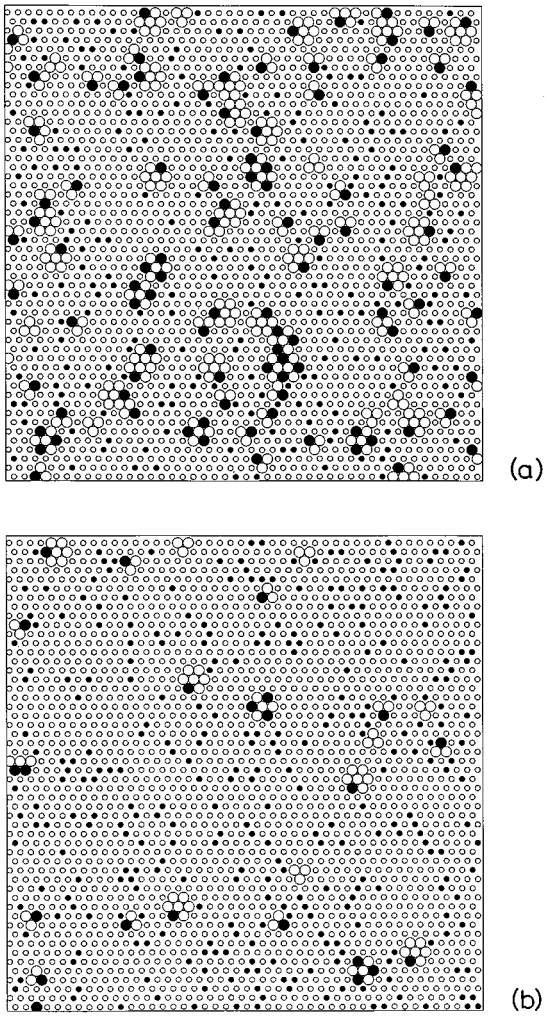

FIG. 3. (111) planes of Ag–13.4 at. % Al for (a) a modeled short-range-ordered alloy and (b) a sample with a random arrangement. Atoms belonging to the $C9$ configuration are shown by enlarged symbols. ○, Ag and ●, Al atoms.

diffuse maxima, 27 values of α_{lmn} (with $R=0.03$, $\chi^2=0.93$) were finally used. Table I gives the values of the Warren-Cowley short-range-order parameters, the recalculated short-range-order scattering is shown in Fig. 2. Both evaluation schemes closely agree. The values of α_{000} deviate by less than ±3% from unity. The magnitude of α_{110} is only 50% of the maximum permitted, $|1-c_{\mathrm{Ag}}^{-1}|=0.154$, reflecting the low degree of short-range order.

Short-range-order parameters were also determined by Kulish and Petrenko.[3] For the sample closest to the one of this investigation, Ag–15 at. % Al quenched from 673 K after aging for 10 min, the data were $\alpha_{110}=-0.08$, $\alpha_{200}=0.24$, $\alpha_{211}=-0.08$, and $\alpha_{220}=0.18$. Only for α_{110} this set agrees with the α_{lmn} of Table I, while for α_{200} and α_{211} the signs are different, and for α_{200} and α_{220} the large positive values are striking. Differences in the sets of α_{lmn} from single crystalline and polycrystalline alloys were previously observed in Cu-rich ^{65}Cu-Zn,[28] where a satisfactory agreement was found only for α_{110}. High correlations in the determination of α_{lmn} from different shells (values close to ±1 in the covariance matrix) observed in the case of diffuse scattering from polycrystals, point to the general problem to

TABLE II. Configuration abundances and enhancement factors with respect to a statistically uncorrelated Ag–13.4 at. % Al alloy for Al around Ag atoms in the first neighboring shell.

Structure	Configuration	Abundance in %	Enhancement factor
A_5B	$C4$	6.2	2.5
	$C5$	20.6	2.0
	$C9$	2.1	3.8
$D0_{22}$	$C16$	0.02	0.5
	$C7$	1.0	1.2
	$C3,C4$	11.8	1.6
	$C17$	0.1	1.7
	$C8$	3.2	2.1
	$C3,C5$	26.2	1.7
Pt_2Mo	$C8$	3.2	2.1
	$C3,C5$	26.2	1.7

deduce meaningful data from polycrystals within such a restricted range of scattering vectors. A further difference between the present data and those of Ref. 3 is readily visible in I_{SRO}. If one calculates short-range-order scattering from a polycrystalline sample within $0.4<|\underline{h}|<1.6$ (the experimental range in Ref. 3) with the data of Table I, a different topology is found as there is a diffuse peak not only around $|\underline{h}|\approx 0.9$ but also at ≈ 1.4. No reason for this difference is known.

LOCAL ATOMIC ARRANGEMENTS

Short-range order in real space was visualized on crystals of $32\times32\times32$ fcc unit cells. They were generated by interchanging A and B atoms till the final arrangement in the crystal was compatible with the given pair-correlation function. As an illustration, Fig. 3 shows (111) planes of modeled crystals with a short-range ordered and a statistically uncorrelated arrangement. The subtle differences reflect the low degree of order. The crystals were then analyzed with respect to the 144 distinguishable atomic configurations of the first coordination shell (Clapp configurations[29]), considering the case of minority atoms around majority atoms. The result is given in Table II in terms of the abundances of a selected number of configurations (Fig. 4) in the short-range-ordered alloy and their respective enhancement factors when referring to a random arrangement. The largest enhancement is found for the $C9$ configuration. Atoms belonging to this configuration are shown by enlarged symbols in Fig. 3.

Table II summarizes the cases of ground-state structures suggested by Asta[8] for the fcc lattice: Ag_5Al (A_5B structure with $C4$, $C5$, and $C9$ as characteristic configurations), Ag_3Al ($D0_{22}$ structure with the $C16$ and $C17$ configurations), and Ag_2Al (Pt_2Mo structure with the $C8$ configuration). With respect to the composition of the alloy investigated, it will be nearly stoichiometric for A_5B, but distinctly understoichiometric for $D0_{22}$ or Pt_2Mo. This was considered by also analyzing the situation in which minority atoms are successively replaced by majority atoms. Table II shows that the best candidate for a ground-state structure is A_5B. This conclusion is further supported if one considers the fraction of the

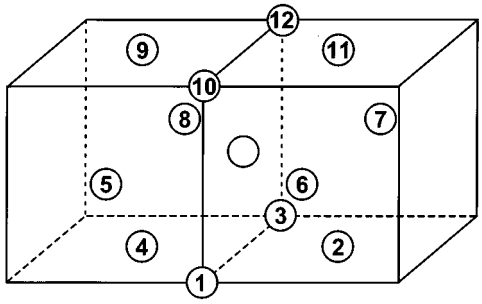

FIG. 4. Nomenclature of configurations as introduced by Clapp (Ref. 29) for the first coordination shell of an atom (open circle) in the fcc structure.

Configuration	Sites occupied by one atom type
$C3$	6,7
$C4$	5,7
$C5$	6,12
$C7$	5,6,7
$C8$	5,6,12
$C9$	1,7,9
$C16$	5,6,7,8
$C17$	4,6,7,9

$C4$, $C5$, and $C9$ configurations in A_5B and in the short-range-ordered alloy. To approach the relation $C4{:}C5{:}C9 = 1{:}2{:}2$ of the long-range-ordered alloy, the enhancement factors of the $C5$, $C4$, $C9$ configurations must increase in this sequence. This is, in fact, observed for the short-range-ordered alloy.

If one only considers nearest neighbors around majority atoms within a {111} plane, the three minority atoms of the $C9$ configuration are found within a single {111} plane. This configuration with an abundance of 0.7% in the short-range-ordered alloy, also has a distinct enhancement factor (of 2.2). This planar configuration is no longer restricted to the fcc lattice, but can also be discussed for the hcp lattice. Two models have been suggested for the ground-state structure of the hexagonal δ phase. In Neumann's model[10] the planar configuration just introduced is the basic building element, while in the model of Howe *et al.*[11] either no minority atom or only minority atoms are located around a majority atom. For the situation of no minority atom around a majority atom, an abundance of 36.5% and an enhancement factor of 0.9 is found. Thus, the present abundance analysis is only consistent with Neumann's model.

The model of Howe *et al.*[11] is supported by first-principles electronic structure calculations for the Ag_2Al stability.[12] Diffuse scattering experiments within the hexagonal δ phase are required to clarify this point. Such measurements are presently under way.

EFFECTIVE PAIR-INTERACTION PARAMETERS

For a canonical ensemble the Hamiltonian H per atom of a binary A-B alloy is written as

$$H/N = c_A c_B \sum_{lmn} V_{lmn}\alpha_{lmn}, \tag{4}$$

TABLE III. Effective pair-interaction parameters V_{lmn} as obtained by the inverse Monte Carlo method with the α_{lmn} of the GC evaluation scheme (Table I).

lmn	V_{lmn} (meV)
110	48.2(5)
200	28.1(3)
211	4.8(2)
220	−0.7(1)
310	4.3(3)
222	−1.0(2)
321	0.6(3)
400	6.3(6)
330	1.0(2)
411	3.1(3)
420	1.5(3)
233	−1.6(1)
422	0.4(2)
431	−0.6(1)
510	2.1(5)
521	0.3(2)
440	−0.1(2)
433	−0.9(2)

where $V_{lmn}=1/2(V_{lmn}^{AA}+V_{lmn}^{BB})-V_{lmn}^{AB}$ are the effective pair-interaction parameters. The set of α_{lmn} in Table I (GC separation technique) was used to determine the V_{lmn} by the inverse Monte Carlo method.[30] Virtual exchanges ($\sim$19 000) were considered on crystals of 64^3 atoms using linear boundary conditions. Results for V_{lmn} were averaged over four modeled short-range-order crystals compatible with the experimental α_{lmn} and their standard deviations. Varying systematically the number of relevant V_{lmn}, a set of 14 is at least required to reproduce the topology of short-range-order scattering with diffuse maxima at $2k_F^{110}$ and 1/2 1/2 1/2 positions in a subsequent Monte Carlo simulation. A set of 18 V_{lmn} was finally taken for a good reproduction of the set of α_{lmn} from experiment. Among the set of V_{lmn} the first two are dominant and positive. Their ratio V_{200}/V_{110} of 0.6 is just within the range of 0.5 to -1 for two significant parameters and diffuse maxima at 1/2 1/2 1/2,[31] and close to the region with diffuse maxima at 1 1/2 0, i.e., reflecting the local $2k_F^{110}$ maxima.

Starting from a long-range-ordered A_5B crystal and using the effective pair-interaction parameters V_{lmn} of Table III, the order-disorder transition temperature was estimated by Monte Carlo simulations. As expected from the low degree of short-range order, a low transition temperature of $\sim$135 K ($\pm$10 K estimated) is obtained. This value is not too different from the ordering temperature obtained in the electronic-structure calculations of Asta and Johnson[8] ($\sim$220 K). Yu *et al.*[32] found a much higher value ($\sim$400 K).

COMPARISON WITH THE Cu-Pt SYSTEM

The simultaneous presence of $2k_F^{110}$ and 1/2, 1/2, 1/2 maxima in short-range-order scattering has also been observed in solid solutions of Cu-Pt. Recently, this system has been studied in detail by Saha and Ohshima[33] for solid solutions with 7–75 at. % Pt. From diffuse x-ray scattering, sets of Warren-Cowley short-range-order parameters were obtained. As long-range-ordered structures are known for Cu-Pt (for the Pt-rich alloys, see Ref. 34), the opportunity is given to analyze the data of Ag-Al also with respect to the building elements of these long-range-ordered structures. In terms of nearest-neighbor configurations of minority atoms around majority atoms these are $C16$ for Cu_3Pt ($L1_2$ structure), $C82$ for CuPt ($L1_1$ structure), $C26$, $C82$, and $C83$ for Cu_3Pt_5 in the abundance ratio $C26:C82:C83=3:1:1$, and $C4$ and $C26$ for $CuPt_3$ with the abundance ratio $C4:C26=1:2$. An abundance analysis of Clapp configurations is presented in Table IV; the data from Cu–32 at. % Pt were not used as it was not possible to model a short-range-ordered alloy with the published set of Warren-Cowley short-range-order parameters. The following conclusions can be drawn.

TABLE IV. Enhancement factors of short-range-ordered Cu–16 at. % Pt, Cu–24.5 at. % Pt, and Cu–75 at. % Pt (see Ref. 33) with respect to a statistically uncorrelated alloy of the same composition for minority around majority atoms in the first neighboring shell.

		Enhancement factor		
Structure	Configuration	16 at. % Pt	24.5 at. % Pt	75 at. % Pt
$L1_2$	$C16$	4.1	17.1	0.5
$L1_1$	$C82$	0.	0.5	0.
Cu_3Pt_5	$C26$	1.8	2.4	3.0
	$C82$	0.	0.5	0.
	$C83$	0.	0.6	0.
$CuPt_3$	$C4$	3.1	1.4	3.1
	$C26$	1.8	2.4	3.0

(i) For Cu–16 at. % Pt and Cu–24.5 at. % Pt, the configuration $C16$ (Cu_3Pt) is enhanced the most, especially in the case of close stoichiometry. Also configurations generated by adding one minority atom at any position of the nearest-neighbor shell ($C34$) or removing one ($C7$) are strongly enhanced. On the Pt-rich side, $C16$ is not enhanced (note that the $2k_F^{110}$ splitting around 100 positions is not observed with dilute Pt-rich or dilute Cu-rich alloys, and only 100 maxima are found). No enhancement of $C16$ is observed for Ag–13.4 at. % Al.

(ii) For Cu–75 at. % Pt, the configurations $C4$ and $C26$ ($CuPt_3$) are most strongly enhanced while adding and/or removing one minority atom of the nearest-neighbor shell yields configurations with enhancement factors of $\sim$1. On the Cu-rich side, $C26$ is also enhanced. For Ag–13.4 at. % Al an enhancement of $C4$ is observed.

This mixture of $C16$ and $C4$, $C26$ configurations in Cu-Pt alloys is consistent with the suggestion of two ''types'' of short-range order introduced by Saha and Ohshima[33] in terms of two pair-correlation functions that should reflect correlations between consecutive (111) layers and because of Fermi-surface imaging. Experiments for solid solutions closer to the stoichiometry of CuPt and Cu_3Pt_5 may help to understand why the configurations $C82$ and $C83$ are not enhanced.

For the present case of Ag–13.4 at. % Al there is no need for two ''types'' of correlations. Only the configurations $C4$, $C5$, $C9$ indicative of one ordered structure (A_5B) are en-

hanced. As neither the configurations $C16$ (Cu_3Pt) nor $C26$ ($CuPt_3$) are enhanced in the short-range-ordered alloy, there is no reason to expect one of the ground states of the Cu-Pt system for fcc Ag-Al.

One might think to get further indications on ordered ground states from diffuse scattering of alloys in the cubic μ phase. Presently, this structure is noted ''disordered'' in the literature as no diffuse scattering experiments have been performed.[35] The problem with such experiments is obvious: the complex structure of the μ phase, the cubic $A13$ structure with 20 atoms per unit cell, will render a detailed analysis and any separation of short-range-order scattering extremely difficult. If nearest-neighbor configurations are obtained, any transfer to the fcc alloy investigated would remain questionable. Diffuse scattering from the hexagonal δ phase currently under way will most probably provide a more direct approach in assessing possible ground-state structures in fcc Ag-Al.

ACKNOWLEDGMENTS

The authors are grateful to E. Fischer for growing the single crystal used in the experiment, and to Dr. M. D. Asta and Dr. D. D. Johnson for discussions and communicating results prior to publication. Financial support by the Swiss National Science Foundation is gratefully acknowledged.

[1] P. S. Rudman, as cited by P. A. Flinn, Phys. Rev. **104**, 350 (1956).
[2] R. I. Bagdasaryan, V. I. Iveronova, A. A. Katsnelson, V. M. Silonov, and M. M. Khrushchov, Izv. Akad. Nauk Arm. SSR, Fiz. **10**, 372 (1975).
[3] N. P. Kulish and P. V. Petrenko, Phys. Status Solidi A **120**, 315 (1990).
[4] S. P. Gupta, Mater. Sci. Eng. **10**, 341 (1972).
[5] W. Pfeiler, P. Meisterle, and M. Zehetbauer, Acta Metall. **32**, 1053 (1984).
[6] A. Malik, B. Schönfeld, G. Kostorz, and J. S. Pedersen, Acta Mater. **44**, 4845 (1996).
[7] G. Kostorz, in *Physical Metallurgy*, edited by R. W. Cahn and P. Haasen (North-Holland, Amsterdam, 1996).
[8] M. D. Asta, as cited by D. de Fontaine, MRS Bull. **21**, 16 (1996); see also M. D. Asta and D. D. Johnson, Comput. Mater. Sci. **8**, 64 (1997).
[9] F. Ducastelle, *Order and Phase Stability in Alloys* (North-Holland, Amsterdam, 1991).
[10] J. P. Neumann, Acta Metall. **14**, 505 (1966).
[11] J. Howe, U. Dahmen, and R. Gronsky, Philos. Mag. A **56**, 31 (1987).
[12] C. L. Rohrer, R. W. Hyland, Jr., M. E. McHenry, and J. M. MacLaren, Acta Metall. **43**, 2097 (1995).
[13] F. Foot and E. R. Jette, Trans. Metall. Soc. AIME **143**, 151 (1941).
[14] J. M. Cowley, J. Appl. Phys. **21**, 24 (1950).
[15] B. Borie and C. J. Sparks, Acta Crystallogr. Sect. A **27**, 198 (1971).
[16] P. Georgopoulos and J. B. Cohen, J. Phys. (Paris), Colloq. **38**, C7-191 (1977).
[17] P. Meisterle and W. Pfeiler, Acta Metall. **31**, 1543 (1983).
[18] D. T. Cromer, J. Chem. Phys. **50**, 4857 (1969).
[19] D. T. Cromer and J. B. Mann, J. Chem. Phys. **47**, 1892 (1967).
[20] L. Quimby and P. M. Sutton, Phys. Rev. **91**, 1122 (1953).
[21] M. A. Krivoglaz, *Theory of X-Ray and Thermal-Neutron Scattering by Real Crystals* (Plenum Press, New York, 1969).
[22] P. A. Doyle and P. S. Turner, Acta Crystallogr. Sect. A **24**, 390 (1968).
[23] S. Sasaki (unpublished).
[24] P. Bardhan and J. B. Cohen, Acta Crystallogr. Sect. A **32**, 597 (1976).
[25] K. I. Ohshima, D. Watanabe, and J. Harada, Acta Crystallogr. Sect. A **32**, 883 (1976).
[26] S. Lefebvre, F. Bley, M. Bessiere, M. Fayard, M. Roth, and J. B. Cohen, Acta Crystallogr. Sect. A **36**, 1 (1980).
[27] F. Klaiber, B. Schönfeld, and G. Kostorz, Acta Crystallogr. Sect. A **43**, 525 (1987).
[28] L. Reinhard, B. Schönfeld, G. Kostorz, and W. Bührer, Phys. Rev. B **41**, 1727 (1990); (unpublished).
[29] P. C. Clapp, Phys. Rev. B **4**, 225 (1971).
[30] V. Gerold and J. Kern, Acta Metall. **35**, 393 (1987).
[31] P. C. Clapp and S. C. Moss, Phys. Rev. **171**, 754 (1968).
[32] J.-Z. Yu, M. Sluiter, and Y. Kawazoe, Sci. Rep. Res. Inst. Tohoku Univ. A **41**, 153 (1996).
[33] D. K. Saha and K.-I. Ohshima, J. Phys.: Condens. Matter **5**, 4099 (1993).
[34] R. Miida and D. Watanabe, J. Appl. Crystallogr. **7**, 50 (1974).
[35] W. B. Pearson, *A Handbook of Lattice Spacings and Structures of Metals and Alloys* (Pergamon Press, New York, 1958); see also S. Fagerberg and A. Westgren, Metallwirtsch. **14**, 265 (1935).